32nd URSI GASS, Montreal, 19-26 August 2017

Solar effects on the Global Atmospheric Electric Circuit

J. C. Tacza* (1), J.-P. Raulin(1), and M. C. De Juli(1)
(1) Center of Radioastronomy and Astrophysics Mackenzie (CRAAM), Engineering School, Mackenzie Presbyterian University, São Paulo, SP, Brazil.

Abstract

Geophysical disturbances as solar flares and energetic particles events, as well as geomagnetic storms are potential candidates to affect the Global Atmospheric Electrical Circuit (GAEC). One can study these effects through measurements of the atmospheric electric field (AEF) in fair weather regions. In this study we investigate the AEF daily curve departures from the standard curve during solar events such as solar flares, solar proton events and Forbush decrease. In some cases, the superposed epoch analysis was utilized. AEF data corresponds to the period between January 2010 - December 2015, and were recorded at Complejo Astronomico El Leoncito (CASLEO). The results show possible ionization effects in regions of disturbed and fair weather, which alters the GAEC.

1. Introduction

The atmospheric electric field (AEF) persists in regions of fair weather (FW). Measures recorded in the oceans showed a diurnal variation, in Universal Time. This diurnal variation is known as the Carnegie curve and is related to the Global Atmospheric Electric Circuit (GAEC) [1].

GAEC is formed between the Earth's surface and the ionosphere and links charge separation in disturbed weather regions with current flow in FW regions [2]. Solar effects and their relationships with the dynamics of the GAEC have been studied indirectly monitoring the departures from the AEF in FW [3]. Such effects include solar flares [4,5], solar proton events (SPE) [6,7] and Forbush decrease [8]. However, the results are ambiguous and the mechanisms are not well defined.

In this paper, we study the variations of AEF during solar flares, SPE and Forbush decrease in order to provide a better understanding of the solar-terrestrial electrical coupling mechanisms. AEF data corresponds to the period between January 2010 - December 2015, and were recorded at CASLEO (Lat. 31.798°S, Long. 69.295°W, Altitude: 2552 masl).

2. Instrumentation and Data Analysis

Continuous measurements of AEF are recorded with two sensors located in CASLEO (CAS1 and CAS2), ~0.4 km apart. Each sensor consists of a commercially manufactured (Boltek Corporation EFM100-1000120-050205) electric field mill (EFM) and are part of a network of similar electric field sensors installed in South America [9]. The dynamic range of the EFM is ±20 kV/m and the response time 0.1 s. The principle of EFM operation is based on the fundamental laws of electromagnetism. When a conducting plate is exposed to an electric field, a charge is induced proportional to its intensity and to the area of the plate. Electric field measurements are recorded with a time resolution of 0.5 s. The electric field intensities are previously corrected to account for the height of the local sensor mounting, which otherwise would result in overestimated readings [9].

The methodology adopted follows the steps described below. First, we calculate monthly mean curves of the diurnal variations of the AEF in FW (standard curve). Our definition of FW is not related to meteorological variables, since there is no weather station close to the EFM location. The criteria for choosing days of FW was to select days with AEF variations in the range of 40-250 V/m. Second, the standard curves were compared with AEF daily curves during the solar events. Third, we may use the superposed epoch analysis (SEA) in order to enhance weak effects. The SEA rely on selecting subsets of data (in our case the AEF daily curve minus the standard curve), wherein key events (start of solar event) in time can be identified. Through the accumulation and averaging of successive key events, the stochastic background variability may be reduced to a point where low-amplitude signals become identifiable [10]. The SEA has been frequently employed to examine a hypothesized link between atmospheric electric properties and solar events [4,8].

3. Results

In the following subsections we describe variations of AEF during different events such as solar flares, SPEs and Forbush decrease.

3.1 Solar Flares

Figure 1 shows the comparison between the X-ray flux and the variations in the AEF during a major solar flare on 29 October 2013. During the solar flare no significant evidence of a variation in the AEF is found. For further analysis, we use the SEA technique (Figure 2) as described above. Figure 2 shows the result for 187 key events none

of them associated with a SEP. No significant effects on the AEF recorded values during solar flares were found.

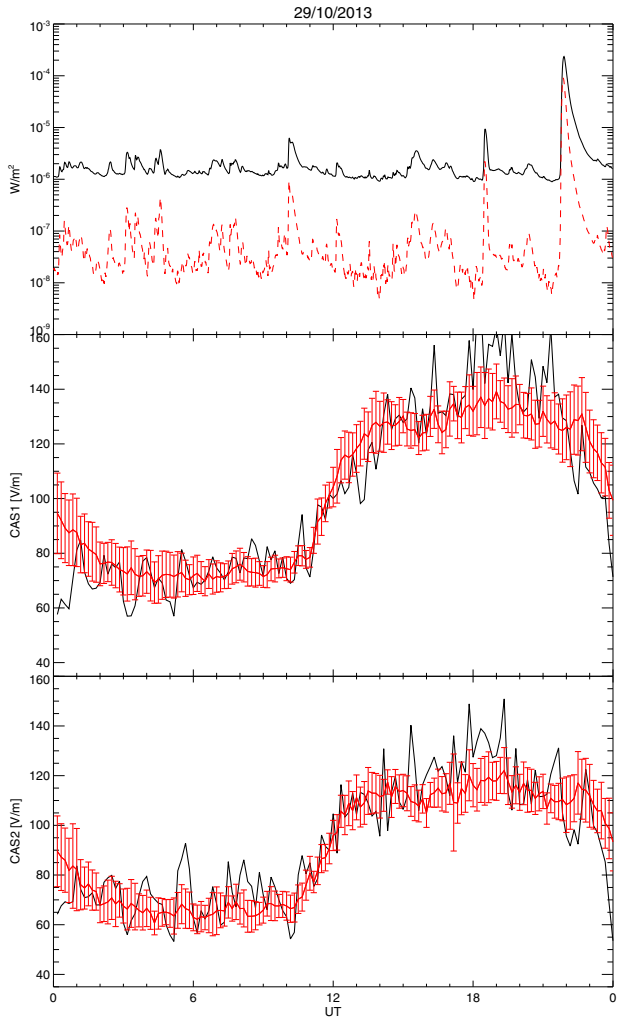

Figure 1. Top: X-ray flux in the bands 0.5-4 Å (dotted line red) and 1-8 Å (solid black line), averaged every 10 minutes. Middle: The black curve represents the CAS 1 AEF daily variation for the day of the solar flare. The red curve represents the AEF monthly average curve of FW days with their respective error bars of 1σ. Both curves were averaged every 10 minutes. Bottom: Same as middle panel for the CAS2 station data.

3.2 Solar Proton Events

As done for solar flares, we analysed SPEs effects on the variations of AEF. Figure 3 compares the proton flux and the AEF values for May 17, 2012. It is important to mention that this SPE produced a Ground Level Enhancements (GLE). We note in Figure 3 that during the increase of the proton flux till its maximum a significant decrease of the AEF recorded values is observed. After about 6 hours, the AEF values increase with respect to mean values. It is worth to mention that these variations are similar in both sensors.

For further analysis, we have used the SEA method (Figure 4). We selected the most intense events, for a total of 8 key events. We observed a small (~ 1 standard error) increase between 0 – 12 hours after the start of the SPE.

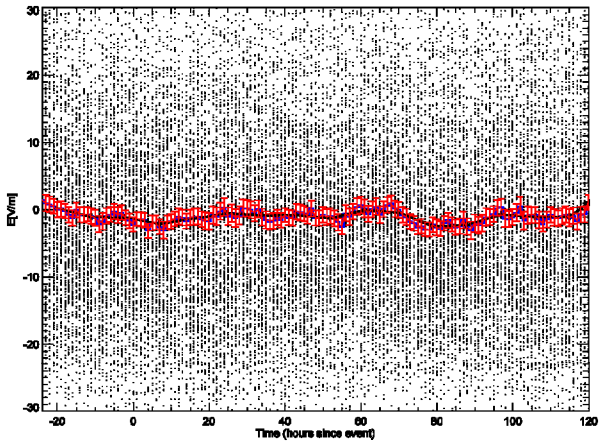

Figure 2. SEA plot showing the AEF average hourly departure from the standard curve (blue line) before and after solar flares recorded at CAS2 station. The solid black line represents an average every 9 hours . The error bars represent two standard error on the mean. The individual dots represent AEF hourly averages departures from the mean value for each subset data. 187 key events were used to create this plot.

3.3 Forbush decrease

The variation of AEF during a very intense geomagnetic storm is shown in Figure 5. This figure shows the DST index variation (top) for the period from 20 May to 19 July 2015 where the zero-time axis indicates 23 June 2015 when DST index reached ~ -200 nT. It is important to note that this intense storm did produce a Forbush decrease (of ~ few percent) recorded at CASLEO by our CARPET charged particle detector [11]. In the middle graph we show the AEF hourly variation for the same period (black curve) and the AEF 24-hours averaged variation (red curve). We note high AEF values corresponding to the minimum DST index but on the same level as increases on the previous days. However, a clear long-term modulation of AEF is observed on both sensors time profiles. The smoothed green curve does represent this modulation. The blue curve is the AEF time profile once the long-term modulation (green curve) is removed, and the superimposed red curve shows its 24-hour average. The latter indicates high AEF values (~35 V/m) at the maximum time of the geomagnetic storm. We observe the same variations for the CAS2 station (bottom). The rapid variations observed days later (day 20) correspond to the presence of lightning close to the EFM sensors.

4. Discussions

In this paper we show results on the AEF variations due to solar flares, SPEs and a very intense geomagnetic storm simultaneously with the presence of a Forbush decrease. For the solar flares analysis, no significant changes of the AEF values were found. Therefore, the most simple explanation, is that the change of electrical conduction particles density during the solar flare due to extra-ionization, is negligible compared with the instantaneous and continuous seed of the electrical potential on the upper boundary of the GAEC.

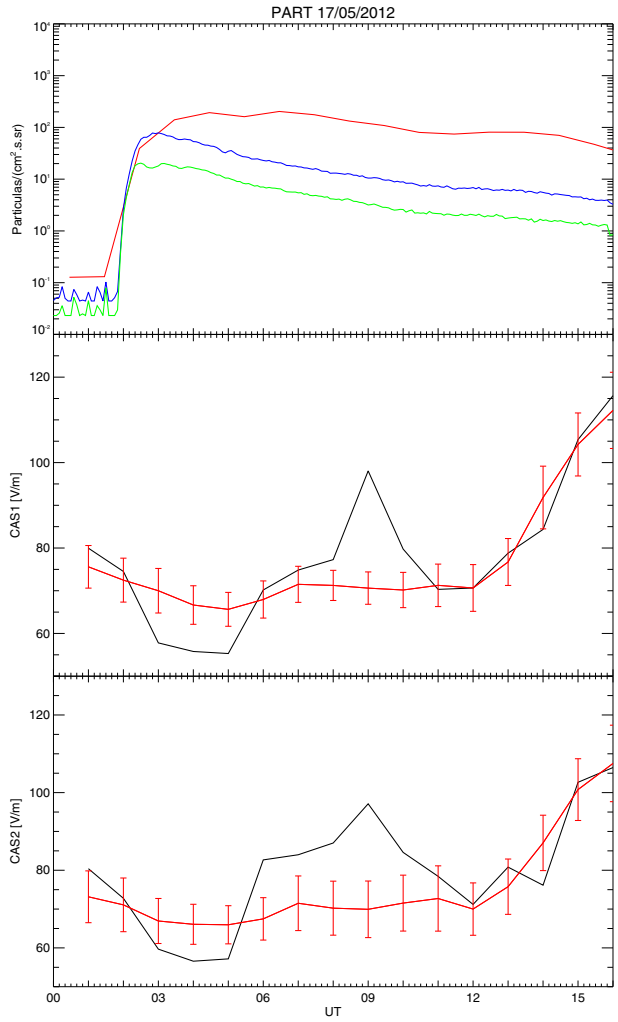

Figure 3. Top: Energy protons flux in the channels > 10 MeV (red color), > 50 MeV (blue color) and > 100 MeV (green color), averaged every 60 minutes. Middle: The black curve represents the CAS1 AEF daily variation for the day of the event. The red curve represents the AEF monthly average curve of FW days with their respective error bars of 1σ. Both curves were averaged every 60 minutes. Bottom: Same as middle panel for the CAS2 station data.

On the other hand, the SPEs analysis shows a significant effect on the AEF values. Figure 3 shows a 2-hour decrease of AEF values at the same time of maximum increase of proton flux. After that (~6 hours later), an increase is noted. These opposite variations may be due to two different physical processes. Excess of precipitating protons during a SPE or lack of precipitating protons during a Forbush decrease may led to changes in the atmospheric electrical conductivity. First, we investigate the decrease of the AEF values. During the SPE there is an increase of ionization producing a high conductivity and, a reduction of AEF is expected, such as shown in figure 3.

The second effect corresponds to an increase on the AEF values. This variation is also found statistically significant when using the SEA technique for all the other SEPs (Figure 4). These results are consistent with the model proposed by Farrell and Desch [7], which suggests that SPEs can increase atmospheric conductivity above electrical storms (disturbed weather regions). This allows more current to flow upstream to the GAEC and thus increase the AEF in FW regions. However, we did not observe a significant decrease on the AEF values as observed in Figure 3 at the beginning of the SPE event. This may be due to the fact that the SEP of May 17, 2012 was the only that produced a GLE event during the studied period. The SPEs included on the SEA technique were intense but not enough to cause changes in the ionization of the atmosphere.

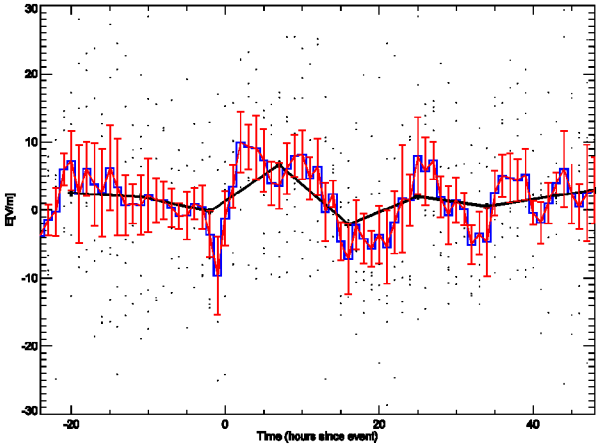

Figure 4. SEA plot showing the AEF average hourly departure from standard curve (blue line) before and after SPEs recorded at CAS2 station. The solid black line represents an average every 9 hours . The error bars represent two standard error on the mean. The individual dots represent AEF hourly averages departures from the mean value for each subset data. 8 key events were used to create this plot.

As for the result shown in Figure 5, we note that a Forbush decrease causes a loss of precipitated charged particles, reducing the ionization and producing a low conductivity and, in this case, an increase on the AEF is expected, such as found here.

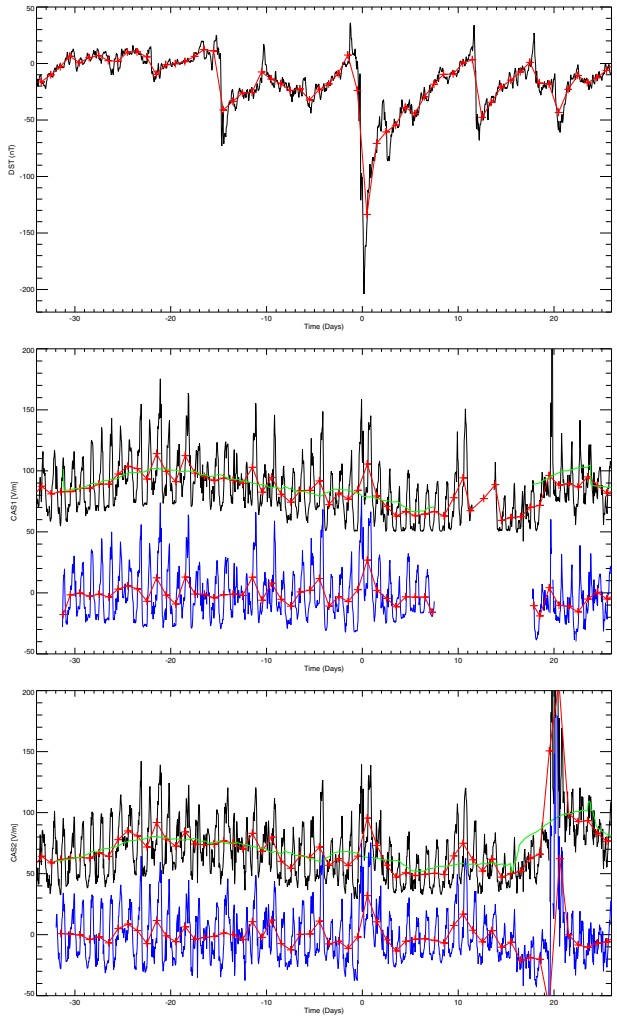

Figure 5. Top: Time variation of the DST index for the period from 20 May to 19 July 2015. Zero time indicates 23 June 2015. Middle: The black color curve represents the CAS1 AEF hourly variation for the study period. The red curve represents the AEF averages every 24 hours. The green color curve represents a running mean (five days). The blue color curve represents the black curve minus the green curve. Bottom: Same as middle panel for the CAS2 station data.

5. Conclusions

In this paper we investigated the effect of solar events on the GAEC through AEF variations in FW regions. No significant effect was found on the AEF values during solar flares. However, very intense events (GLE and Forbush decrease) can produce changes on the ionization which modifies the atmospheric conductivity and, therefore, altering the AEF in FW regions. Also, SEPs can modify the conductivity in areas of electrical storms (disturbed weather regions) affecting the GAEC in FW regions.

6. References

1. R. G. Harrison, "The Carnegie curve", Surveys in Geophysics, 34, 2, December 2012, pp. 209-232, doi: 10.1007/s10712-012-9210-2.
2. M. J. Rycroft, R.G. Harrison, K. A. Nicoll and E.A. Mareev, "An overview of Earth's global electric circuit and atmospheric conductivity", Space Science Reviews, 137, 1-4, May 2008, pp. 83-105, doi: 10.1007/s11214-008-9368-6.
3. M. J. Rycroft, K. A. Nicoll, K. L. Aplin and R. G. Harrison, "Recent advances in global electric circuit between the space environment and the troposphere", Journal of Atmospheric and Solar-Terrestrial Physics, 90-91, December 2012, pp. 198-211, doi: 10.1016/j.jastp.2012.03.015.
4. W. E. Cobb, "Evidence of a solar influence on the atmospheric electric elements at Mauna Loa Observatory", Monthly Weather Review, 95, 12, December 1967, pp. 905-911.
5. R. Reiter, "Further evidence for impact of solar flares on potential gradient and air-earth current characteristics at high mountain stations", Pure and Applied Geophysical, 86, 1, May 1970, pp. 142-158, doi: 10.1007/BF00875081.
6. K.A. Nicoll and R.G. Harrison, "Detection of lower tropospheric responses to solar energetic particles at midlatitudes", Physical Review Letters, 112, June 2014, pp. 225001 (1-5), doi: 10.1103/PhysRevLett.112.225001.
7. W. M. Farrel and M. D. Desch, "Solar proton events and the fair weather field at ground", Geophysical Research Letters, 29, 9, May 2002, pp. 37 (1-4), doi: 10.1029/2001GL013908.
8. D. W. Engfer, B. A. Tinsley, "An investigation of short-term solar wind modulation of atmospheric electricity at Mauna Loa Observatory", Journal of Atmospheric and Solar-Terrestrial Physics, 61, September 1999, pp. 943-953, doi: 10.1016/S1364-6826(99)00057-7.
9. J. C. Tacza, J.-P. Raulin, E.L. Macotela, G. Fernandez, E. Correia, M. J. Rycroft and R. G Harrison, "A new South American network to study the atmospheric electric field and its variations related to geophysical phenomena", Journal of Atmospheric and Solar-Terrestrial Physics, 120, December 2014, pp. 70-79, doi: 10.1016/j.jastp.2014.09.001.
10. B.A. Laken and J. Calogovic, "Composite analysis with Monte Carlo methods: an example with cosmic rays and clouds", Journal of Space Weather and Space Climate, 3, September 2013, pp. A29(1-13), doi: 10.1051/swsc/2013051.
11.R.R.S. De Mendonça, J.-P. Raulin, F.C.P. Bertoni, E. Echer, V.S. Makhmutov, G. Fernandez, "Long-term and transient time variation of cosmic ray fluxes detected in Argentina by CARPET cosmic ray detector", Journal of Atmospheric and Solar-Terrestrial Physics, 73, July 2011, pp. 1410-1416, doi: 10.1016/j.jastp.2010.09.034.